An application of error reduction and harmonic inversion schemes to the semiclassical calculation of molecular vibrational energy levels

Sharif D. Kunikeev,[a] Erdinç Atilgan, and Howard S. Taylor
Department of Chemistry, University of Southern California, Los Angeles, California 90089-0482

Alexey L. Kaledin[b]
Department of Chemistry and Kenneth S. Pitzer Center for Theoretical Chemistry, University of California, and Chemical Sciences Division, Lawrence Berkeley National Laboratory, Berkeley, California 94720

Jörg Main
Institut für Theoretische Physik 1, Universität Stuttgart, 70550 Stuttgart, Germany

(Received 11 December 2003; accepted 12 January 2004)

A singular value decomposition based harmonic inversion signal processing scheme is applied to the semiclassical initial value representation (IVR) calculation of molecular vibrational states. Relative to usual IVR procedure of Fourier analysis of a signal made from the Monte Carlo evaluation of the phase space integral in which many trajectories are needed, the new procedure obtains acceptable results with many fewer trajectories. Calculations are carried out for vibrational energy levels of H_2O to illustrate the overall procedure. © *2004 American Institute of Physics.*
[DOI: 10.1063/1.1652523]

I. INTRODUCTION

The initial value representation (IVR) of semiclassical (SC) theory has received much attention in recent years.[1–4] Much of the interest in these studies is stimulated by the fact that as compared to the corresponding quantum calculations, the SC calculations scale more favorably with increasing degrees of freedom. It is desired to develop a practical SC method capable of calculating problems in challenging multidimensional molecular dynamics including quantum effects. In the SC–IVR, which shows some promise in achieving this goal, the quantum mechanical time evolution operator, $\exp(-i\hat{H}t/\hbar)$, is approximated by an integral operator with the kernel expressed in terms of only classical values and coherent states integrated over the initial values of the momenta and coordinates, $(\vec{p}_0,\vec{q}_0)$, for a classical trajectory of the molecular dynamics problem at hand. The present paper is concerned with the determination of vibrational energy levels of a bound molecular system, which can be conveniently identified as peaks in the spectral density,

$$I(E)=\frac{\mathrm{Re}}{\pi\hbar}\int_0^\infty dt\,\exp(iEt/\hbar)c(t), \tag{1}$$

where $c(t)\equiv\langle\xi|\exp(-i\hat{H}t/\hbar)|\xi\rangle$ is the autocorrelation function or signal with $|\xi\rangle$ being some reference state. The Herman–Kluk[5] (HK) IVR propagator gives the following expression for the autocorrelation function:

$$c(t)=(2\pi\hbar)^{-F}\int d\vec{p}_0\,d\vec{q}_0\langle\xi|\vec{p}_t\vec{q}_t\rangle\langle\vec{p}_0\vec{q}_0|\xi\rangle \times\exp(iS_t(\vec{p}_0,\vec{q}_0)/\hbar)C_t(\vec{p}_0,\vec{q}_0), \tag{2}$$

where F is the dimension of the system; $S_t(\vec{p}_0,\vec{q}_0)$ is the classical action integral along the classical trajectory with the values of the momenta and coordinates at time t, $\vec{p}_t\equiv\vec{p}_t(\vec{p}_0,\vec{q}_0)$ and $\vec{q}_t\equiv\vec{q}_t(\vec{p}_0,\vec{q}_0)$, that evolve from the initial conditions $(\vec{p}_0,\vec{q}_0)$; $C_t(\vec{p}_0,\vec{q}_0)$ is the HK pre-exponential factor;[5] $|\vec{p}_0\vec{q}_0\rangle$ is a coherent state,[6,7] whose coordinate space wave function is given by

$$\langle\vec{q}|\vec{p}_0\vec{q}_0\rangle=\left(\frac{\gamma}{\pi}\right)^{F/4}e^{-\gamma(q-q_0)^2/2+ip_0\cdot(q-q_0)/\hbar}. \tag{3}$$

The main advantage of the HK–IVR approach over the usual SC methods based on the Van Vleck type SC propagators[8] is that it avoids the notoriously difficult root-search problem, in which all possible classical trajectories connecting two points in coordinate space by a certain time interval must be located. To calculate the HK–IVR spectral density, Eqs. (1) and (2), one needs to compute a classical trajectory for each set of initial condition $(\vec{p}_0,\vec{q}_0)$, evaluate the integrand along the trajectory, and then to perform the Fourier transform over t. For systems of many degrees of freedom, the phase space average will be an integral of high dimensionality, so that a Monte Carlo method is the only feasible way to do it. There have been a number of calculations along these lines, most of which have given good results for the vibrational energy levels (or other spectral densities relevant to the photoabsorption cross-section, the photoelectron spectrum, etc.).[9–15] Of concern, however, has been the number of trajectories that must be computed, i.e., the number of initial phase points that must be sampled in Eq. (2), in order to obtain converged results. The more one

[a]Permanent address: Institute of Nuclear Physics, Moscow State University, 119899 Moscow, Russia. Electronic mail: kunikeev@usc.edu
[b]Present address: Department of Chemistry, Cherry L. Emerson Center for Scientific Computing, Emory University, Atlanta, GA 30322.

can do to reduce the number of trajectories that are needed, the more practical the overall approach will be for an application to large molecular systems of interest.

There have been several approaches suggested to improve the efficiency of the IVR phase space average; among them, the Filinov filtering scheme,[16,17] the filter-diagonalization technique,[18] and others.[1] A recent idea is to use time averaging of the integrand, Eq. (2), to get rid of much of the oscillatory behavior of the integrand (sign problem), so that many fewer initial conditions (i.e., trajectories) are needed for the Monte Carlo phase space average to converge.[19,20] Note that all the methods based on the Fourier transform spectral analysis are inherently low resolution methods with resolution being inversely proportional to the length, $T \equiv N\tau$ (τ is the time interval between adjacent time samples) of the signal $c(t)$ so that to get spectral features resolved they need more signal points sampled. This in turn requires more trajectories to be averaged to achieve convergence.

This happens for two reasons: First, the integrand becomes more oscillatory at larger *t*. Second, the HK propagator is a short time propagator. This means that $c(t)$ for a given number of averaged trajectories behaves unphysically at longer times creating more error in the signal. These effects necessitate more trajectories to be averaged in the not always fulfilled hope of reducing the error. Hence it would clearly be advantageous to have a time to frequency processor that can yield acceptable results and resolution using shorter time propagations, i.e., shorter signals. The harmonic inversion (HI) class of processors in its several variants, the filter diagonalization method, (FDM) the linear predictor method, and the Padé method supply such an alternative.[21] All these methods gain their advantage by assuming a model, namely a linear combination of decaying complex exponentials. When such methods are fed by converged signals which are nearly free of error (or noise) they yield excellent and similar results if the harmonic inversion equations are properly regularized.

Reference 18 applied these ideas using FDM to compute resonances (or energies) in collinear H_2+H scattering. Although a systematic study was not given, it was noted that acceptable results were obtained with up to a factor of 16 fewer trajectories than could be obtained using Fourier methods that as explained above invite more error and which can do nothing but signal averaging to reduce the error.

In this paper, in the spirit of Ref. 18 we apply the harmonic inversion method to the IVR signal, Eq. (2), averaged over N_{tr} trajectories to obtain the lower vibrational energies of H_2O molecule. This is a 3D problem that is more challenging than the 1D H_2+H problem. In doing this problem we make several changes in methodology from Ref. 18 two of which are alternatives to the windowing and the method of extracting the energies. FDM does the former by partitioning a localized Fourier–Krylov basis and the latter by diagonalizing the Hamiltonian on Fourier–Krylov basis designed to cover the window. Our method of windowing is explained in Sec. II A and our method of obtaining the energies and weights of the vibrational states in the signal is explained in Sec. III. For the latter we used the previously published Padé method.[21]

Most importantly here we address the problem that the results produced by the harmonic inversion methods are very sensitive to residual signal error in the sense that false error peaks can appear and are often indistinguishable from true peaks, and also if the noise/error is too high, true peaks can be undetected. This serious fault, which did not occur in the simpler H_2+H problem, will be cured here by applying the Cadzow regularization method for error reduction which will be introduced in Sec. II B and also by using different reference states as explained in Sec. IV.

Here, we apply the Cadzow regularization iterative procedure[22] to first reduce the error in the windowed signal. Later by using the HI Padé[21,23] solver we extract vibrational energy levels from the error reduced signal. The error reducing method applied in the present work is the analogue of a noise reducing method used in signal processing of experimental NMR signals.[23] In this sense, this work can be considered as two step processing: First, noise/error reduction of the signal; second, harmonic inversion of the cleaned signal to obtain harmonic inversion parameters or the line list. Atomic units ($\hbar=1$) are used throughout the rest of the paper unless specified otherwise.

II. NOISE/ERROR REDUCTION

A. Windowing

All processing can be done by breaking the Fourier transform spectrum into windows of 100 to 400 (300 is usual) Fourier grid points. The reasons for windowing as done here is that for the noise/error reduction part of the problem: (i) without windowing the so-called singular value decomposition (SVD)[24] graphs, to be discussed below, become too cluttered with signal and noise singular value points to be easily analyzed; (ii) certain windows will be much simpler to process than others, and not windowing unnecessarily ties all features to the features most affected by noise; and (iii) without windowing the dimension $N/2$ of the data matrix arising in the Cadzow method (will be explained in Sec. II B) would be so large that a needed SVD calculation could become too time consuming.

The edges of the windows are at Fourier grid points. Their placement ideally, based on prior knowledge or hints from the noise/error corrupted Fourier transform spectrum, surrounds regions containing signal peaks and begins and ends in regions of pure noise. In less than ideal situations a systematic windowing of the spectrum can be designed for all regions. If peaks, because of spectral density reasons, unavoidably appear at window edges where window induced distortions will occur, an additional window should be chosen so that the edge of the prior window falls interior to the new window. This is possible because windows do not know about each other and can overlap. Choosing windows is generally not a problem and becomes even less so with experience.

At this point the windowing program takes over and produces a signal of length N_w, called c_n^{bl}, "*bl*" for band limited, out of the measured/calculated signal of length N called

c_n. This is inputted into the Cadzow noise reduction scheme described in Sec. II B below. The production process, described with formulas in Ref. 21, is here discussed in words. In the Fourier spectrum of a signal averaged over a given number of trajectories all intensities outside the window of N_w Fourier grid points are set to zero. The window spectrum is then shifted symmetrically about zero frequency (energy) and inverse Fourier transformed to produce a "new" signal. Since the original bandwidth was $2\pi/\tau$ (τ is the sampling or dwell time) and now it is reduced by the factor N_w/N, the new effective sampling or dwell time will be $N\tau/N_w \equiv \tau_w$. Hence the band limited signal with nth element $c_n^{bl} \equiv c^{bl}(n\tau_w)$ is just the "new" signal with fewer samples numbered $n=0,1,...,N_w-1$. As $T \equiv N\tau = N_w\tau_w$, resolution is not affected by this signal length reduction. After all processing the real part of the frequencies (energies) must be shifted back to the original origin. Results near window edges are not reliable.

B. Cadzow regularization

The Cadzow method is based on the general idea to create from a given, nonideal, band limited signal c_n with a signal length N (we dropped superscript "bl" in c_n^{bl} and subscript "w" in N_w and τ_w), which is contaminated by noise or error perturbations, a new signal that satisfies a number of *a priori* known properties of the underlying signal and at the same time is the closest to the original signal. It is assumed that the HK–IVR autocorrelation signal, Eq. (2), can be decomposed as a sum

$$c(t) = x(t) + \epsilon(t), \quad x(t) = \sum_{k=1}^{K} d_k \exp(-iE_k t), \tag{4}$$

where E_k and d_k are the kth vibrational energy level and the weight amplitude; $\epsilon(t)$ is the error due to nonconvergence of the Monte Carlo average, which is scaled as $1/\sqrt{N_{tr}}$ with the number of trajectories N_{tr} taken into the Monte Carlo average. The HI part of the signal $x(t)$ is what we are looking for, while $\epsilon(t)$ is the unwanted part of the signal. The validity of the decomposition Eq. (4) is based on the two facts: First, an exact quantum mechanical autocorrelation function satisfies the HI signal form with the energy E_k and amplitude $d_k = |\langle \Psi_k | \xi \rangle|^2$ defined by the Schrödinger equation, $\hat{H}\Psi_k = E_k \Psi_k$. Second, the HK semiclassical expression Eq. (2) approximates the corresponding quantum mechanical one up to $\hbar$ terms.

Let us assume that the signal is given on an equidistant grid $c_n = c(n\tau)$ and $x_n = x(n\tau)$, $n=0,...,N-1$, and N is assumed to be even. The best that can be done to extract x_n from c_n is to minimize the fitting error,

$$\min_{d_k, E_k} \sum_{n=0}^{N-1} w_n |c_n - x_n|^2 = \min_{d_k, E_k} \sum_{n=0}^{N-1} w_n \left| c_n - \sum_{k=1}^{K} d_k \exp(-iE_k n\tau) \right|^2, \tag{5}$$

where $w_n = 1/s_n^2$ is a weight coefficient inversely proportional to the squared error deviation s_n^2 of the nth data point. In practice, the distribution of the error deviations in time is not known and can be modeled as a uniform or more complicated distribution function. Let us consider minimization of the following error cost function:

$$\min_{d_k, E_k} \|C - X\|_F^2 = M \min_{d_k, E_k} \sum_{n=0}^{N-1} w_n |c_n - x_n|^2, \tag{6}$$

where

$$w_n = \begin{cases} (n+1)/M, & n=0,1,2,...,M-1, \\ 1, & n=M, M+1,...,N-M, \\ (N-n)/M, & n=N-M+1,...,N-1. \end{cases}$$

Here C is the so-called data matrix $C_{nm} = c_{n+m}$ and $X_{nm} = x_{n+m}$, $n=0,1,...,M-1$, $m=0,...,N-M$ and $\|\cdot\|_F$ denotes the Frobenius matrix norm. M can be taken as $N/2$ (small changes are not important[23]) so the data matrix C will be a $N/2 \times (N/2+1)$ rectangular matrix. Obviously, X is a K-rank matrix, but due to random errors C is usually a full-rank matrix. The solution matrix X also satisfies the Hankel property, i.e., elements on the antidiagonals are the same [see Eq. (12)]. Cadzow suggested an algorithm for approximating this solution. Specifically, the original problem Eq. (6) is decomposed into two simpler subproblems related to each of the individual signal property subsets. In the first step, we are looking for a K-rank matrix, $X^{(K)}$, which is the best approximation to the data matrix C,

$$\min_{X \subset R_K} \|C - X\|_F^2, \tag{7}$$

and in the second step, a Hankel matrix is found to minimize

$$\min_{X \subset H} \|X^{(K)} - X\|_F^2. \tag{8}$$

The solution of the first step is well known.[25] For a general full rank complex valued $M \times (N-M+1)$, $M \leqslant (N-M+1)$ matrix C, its associated SVD representation takes the following form:

$$C = X^{(K)} + E^{(M-K)} = \sum_{k=1}^{K} \sigma_k |u_k\rangle\langle v_k| + \sum_{k=K+1}^{M} \sigma_k |u_k\rangle\langle v_k|, \tag{9}$$

where σ_k are the singular values, while $|u_k\rangle$ and $\langle v_k|$ are the left and right singular vectors, respectively. The singular values are here ordered in a monotonically decreasing fashion $\sigma_{k+1} \leqslant \sigma_k$. Zeroing the smallest singular values $\sigma_{K+1} = \cdots = \sigma_M = 0$ or setting $E^{(M-K)} = 0$ in Eq. (9), one gets a K-rank matrix $X^{(K)} = \hat{R}_K C$, where $\hat{R}_K$ denotes a rank reducing (nonlinear) operator transforming $C \to X^{(K)}$.

Estimating the rank, the value of K, is the most essential step in our method. For an ideal converged signal with no error or noise the rank K could easily be spotted as the number of K nonzero singular values. For this case, in SVD graphs, the signal points could be recognized as some decreasing sequence of points while the noise/error points could be distinguished as a horizontal line of almost equally spaced points or a "string of points" close to zero level. If the noise/error level is increased slowly, this effect shows

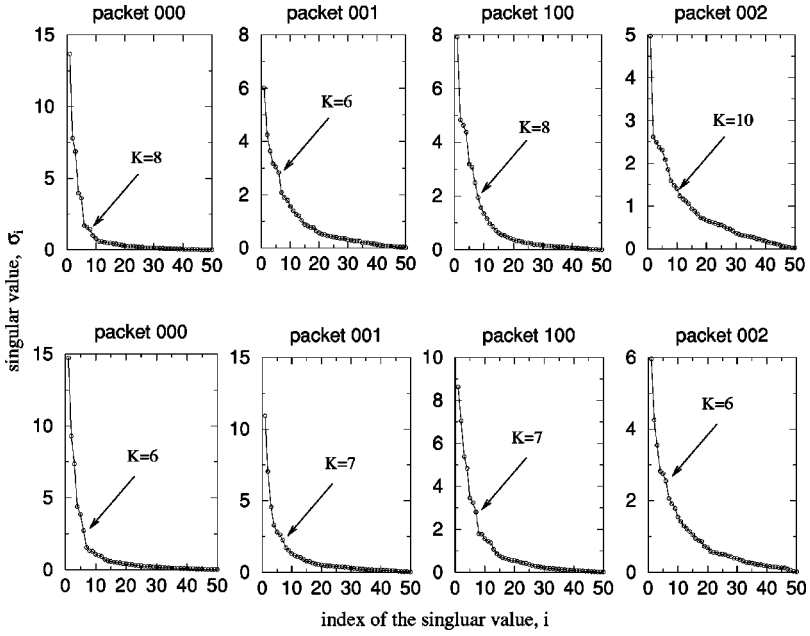

FIG. 1. The singular values of the data matrices for all packets. Upper row graphs belong to A_1 symmetry, and lower row graphs belong to B_2 symmetry.

itself on the SVD graphs as an increase on the height of this horizontal string of points (noise/error points) relative to signal points. If noise/error level is increased more, eventually, some signal points might be covered by the string of points depending on the strength of the noise relative to the signal. Therefore the K value will simply be taken as the number of points above the noise/error points. That is, we will only be interested in the singular values that are well above the noise/error points, and those below the noise/error level, if they exist, will be omitted. The best strategy, up to date, to distinguish the signal points from the noise/error points is to look for a ''gap'' in the SVD graphs. The distance from the highest noise point to the lowest signal point above the highest noise point is defined as the ''gap.'' Figure 1 shows eight different sets of singular value graphs from different packets (will be explained in Sec. IV). The ''gap'' in real cases can be estimated by recognizing that it always appears near ''elbow'' of the curves as in Fig. 1. In many cases, there is a clear separation of signal points from the noise/error points. When the gap is not clear we hold to a conservative strategy and chose a few points more on the elbow by considering a next possible gap towards the region of noise/error points. Even though the noise/error points, ''string of points,'' should theoretically (in case of a white Gaussian distributed noise) be around a constant value, i.e., zero slope, in the SVD graphs, we observe a slight nonzero slope. This is caused by the effect of windowing and possible nonwhite nature of noise/error perturbations, but since the near horizontal character is distinguishable the gap criteria is still applicable.

After the rank reduction operation the Hankel property is lost. The second step is simply to average over the antidiagonal elements or to Hankelize the matrix. The Hankelization can be formulated as $X^{(H)}=\hat{H}X^{(K)}$, where $\hat{H}$ denotes a Hankelization (linear) operator (not to be confused with Hamiltonian operator), is given by

$$X_{ij}^{(H)}=x((i+j)\tau)=\frac{1}{L}\sum_{\substack{n,m:\\ m+n=i+j}} X_{nm}^{(K)}, \tag{10}$$

with L being the number of the elements in matrix $X^{(K)}$ satisfying $m+n=i+j$ in Eq. (10).

These regularization steps have to be applied many times to reach a convergence in the results; that is the procedures should be iterated N_{iter} times until a Hankel matrix $X_{N_{\text{iter}}}^{(H)}=(\hat{H}\hat{R}_K)^{N_{\text{iter}}}C$ with only K dominant singular values is obtained. From the approximated Hankel matrix $X_{N_{\text{iter}}}^{(H)}$, better error-reduced data $x_{N_{\text{iter}}}(n\tau)$ can be read off. The convergence of the above iteration can be proved using the theory of composite property mapping algorithm.[22] Let $X_{\text{true}}=X$ denotes the true underlying data matrix; then, it can be proved[26] that

$$\|X^{(H)}-X_{\text{true}}\|_F\leqslant\|X^{(K)}-X_{\text{true}}\|_F. \tag{11}$$

The equality holds only if $X^{(K)}$ is Hankel. The above inequality demonstrates that $X^{(H)}$ is always more accurate than $X^{(K)}$. If the SVD in the iteration procedures can reduce the error effect efficiently, a better estimation of X_{true} can be obtained by preserving the Hankel form after each iteration. Hence, the performance of the Cadzow preprocessed HI algorithm should be better than that of the original HI algorithm as applied to the signal Eq. (4).

Now, having $x_{N_{\text{iter}}}(n\tau)$, $n=0,...,N-1$ signal, which better satisfies the HI model, one can actually apply any form of the HI algorithm to perform the spectral analysis of the signal with practically the same results on output. In this paper, we have used the Padé HI spectral estimator to get the $\{d_k,E_k\}_{k=1}^{K}$ parameters as described, e.g., in Refs. 21 and 23.

Before proceeding to the next section we give an algorithm summarizing the above error reduction signal processing scheme.

Step 1: Create a matrix C from a windowed signal c_n, $n=0,...,N-1$, as

$$C=\begin{pmatrix} c_0 & c_1 & c_2 & \cdots & c_{N/2} \\ c_1 & c_2 & c_3 & \cdots & c_{N/2+1} \\ c_2 & c_3 & c_4 & \cdots & c_{N/2+3} \\ \cdots & \cdots & \cdots & \cdots & \cdots \\ c_{N/2-1} & c_{N/2} & c_{N/2+1} & \cdots & c_{N-1} \end{pmatrix}. \tag{12}$$

Step 2: Make the SVD of the matrix: $C\rightarrow USV^H$ where U and V are unitary matrices composed from the left and right singular vectors, respectively, and S is a rectangular diagonal matrix with the singular values on the diagonal.

Step 3: For the first iteration ($N_{\text{iter}}=1$), estimate the rank K from the SVD graph. For the following iterations ($N_{\text{iter}}>1$), use the same rank. Given K set to zero all smaller $N/2-K$ singular values: $S\rightarrow S'$.

Step 4: Find a new matrix $C':US'V^H\rightarrow C'$.

Step 5: Do Hankelization.

Step 6: Go to step 2 and replace C by C' in Eq. (12) then iterate the procedure N_{iter} times until the convergence is achieved.

Step 7: From the N_{iter} times iterated matrix C, which is of Hankel form, read off an error reduced signal $x_n^{N_{\text{iter}}}=x_{N_{\text{iter}}}(n\tau)$, $n=0,...,N-1$.

III. PADÉ HI METHOD

The $x_n^{N_{\text{iter}}}$, $n=0,...,N_w-1$, which are hopefully very similar to the exact noiseless signal samples x_n, can be subjected to a harmonic inversion analysis. The spectrum $I(E)$ which can be represented in the infinite discrete Fourier transform (DFT) (or z transform) of the signal described by Eq. (4) can be obtained via

$$\begin{aligned} I(E)&=\tau_w\sum_{n=0}^{\infty} x_n z^{-n} \\ &=\tau_w\sum_{k=1}^{K}\frac{d_k}{1-z_k/z} \\ &=\tau_w\sum_{k=1}^{K}\frac{d_k}{1-\exp[\mathrm{i}(E-E_k)\tau_w]}, \end{aligned} \tag{13}$$

where $z=\exp(-\mathrm{i}E\tau_w)$ and $z_k=\exp(-\mathrm{i}E_k\tau_w)$. The real part of Eq. (13) gives the density spectrum Eq. (1). The right-hand side of Eq. (13), obtained as a result of summing up an infinite series of signal points, is the harmonic inversion spectral estimator expressed in terms of harmonic inversion parameters. If $|(E-E_k)\tau_w|\ll 1$, Eq. (13) reduces to a sum of complex Lorentzians. In the spectral regions far from resonance lines, $\mathrm{Re}\,I(E)=(\tau_w/2)\Sigma_{k=1}^{K}d_k=\tau_w x_0/2$ (if all d_k's are real) so that in order to get zero baseline the constant $\tau_w x_0/2$ should be subtracted from Eq. (13).

Formally let us construct from the signal Eq. (4) an infinite Hankel matrix $x_{nm}=x_{n+m}=x((n+m)\tau)$, $n,m=0,1,...$. Then the matrix x_{nm} has a finite rank K and there exist K numbers $\alpha_1, \alpha_2,\ldots,\alpha_K$ such that

$$x_q=\sum_{k=1}^{K}\alpha_k x_{q-k} \quad (q=K,K+1,...) \tag{14}$$

(see Vol. II, Chap. XV, Sec. 10 in Ref. 27 for proof). The linear prediction (LP) equations (14) enable one to calculate all the signal points knowing the first K signal points and the K LP equation coefficients; the LP coefficients in turn can be obtained as a solution of the system of K LP equations.

If the infinite matrix x_{nm} is of finite rank then the DFT of the signal can be summed up to a rational function of z (Padé approximant),[27]

$$I(E)=\tau_w\sum_{n=0}^{\infty}x_n z^{-n}=\tau_w\frac{P_K(z)}{Q_K(z)}, \tag{15}$$

where $P_K(z)=\Sigma_{k=1}^{K}b_k z^{K-k+1}$ and $Q_K(z)=\Sigma_{k=0}^{K}a_k z^{K-k}$ are, respectively, numerator and denominator polynomials whose coefficients can be calculated from the following system of relations:

$$b_k=\sum_{r=0}^{k-1}a_r x_{k-1-r} \quad (k=1,...,K), \tag{16a}$$

$$0=\sum_{k=0}^{K}a_k x_{q-k} \quad (q=K,K+1,...,2K-1). \tag{16b}$$

Setting $\alpha_k=-a_k/a_0$, $k=1,...,K$, we can write the relations Eq. (16b) in the form Eq. (14). Therefore, the a_k's coefficients can be obtained as a solution of a set of the LP equations,[24] whereas the b_k's ones from the *explicit* relations Eq. (16a).

The harmonic inversion parameters, z_k or E_k, can be found, by rooting the denominator polynomial. This problem can be effectively reduced to the diagonalization of the companion Hessenberg matrix.[21,25] The parameters d_k are calculated via the residues of the Padé approximant Eq. (15) at the positions of the corresponding complex poles z_k.[21]

IV. VIBRATIONAL ENERGY LEVELS OF THE H_2O MOLECULE

To illustrate the overall procedure, calculations for the vibrational energy levels of H_2O are carried out. We use a standard normal mode vibrational Hamiltonian that ignores vibration–rotation coupling[28,29] and a well-studied potential energy surface for which exact quantum-mechanical results have been reported.[30] The $3N-6=3$ normal mode coordinate are mass-weighted in the usual way[19] so that q_1, q_2, q_3 denote mode coordinates for bending, symmetric stretch, and asymmetric stretch vibrations, respectively. The reference state $|\xi\rangle$ is taken to be a coherent state $|\vec{p}_r\vec{q}_r\rangle$, Eq. (3) (with $\gamma_j=\omega_j$), centered at the coordinate (potential energy) equilibrium position $\vec{q}_r=\vec{q}_e$ and the momentum $\vec{p}_r=(p_{r1},p_{r2},p_{r3})$ with component value $p_{rj}=\sqrt{(2n_j+1)\omega_j}$ corresponding to the vibrational energy specified by harmonic oscillator quantum number n_j and normal mode frequency ω_j for $j=1, 2, 3$. According to a specific symmetry of the molecular system, the reference state can be made to have + or − symmetry upon $q_3\rightarrow -q_3$ reflection, which gives a state of A_1 or B_2 symmetry, respectively. The sampling function used for the Monte Carlo average over the

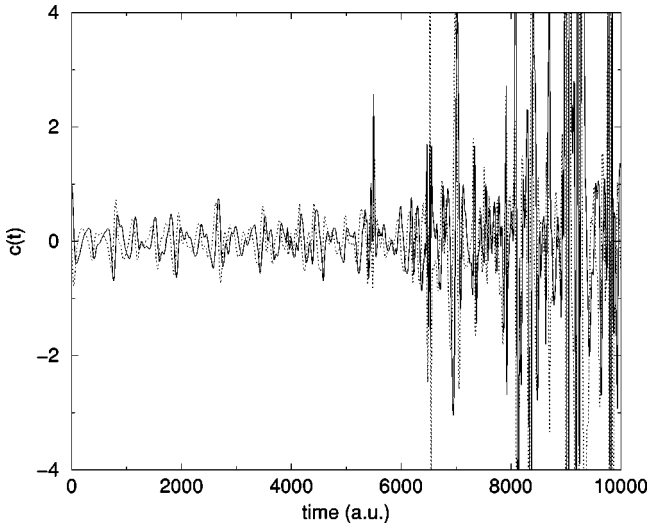

FIG. 2. The SC signal for packet 000 symmetry A_1 obtained by 5000 trajectories. The full line is the real, the dotted line is the imaginary part of the signal.

phase space was the Husimi distribution function[31] as described in Ref. 19. We use a rejection Monte Carlo algorithm combined with the Box–Muller method to select trajectories.[24] The trajectories are propagated for 244 fs (1000 steps, $\tau=10$ a.u.). For details on numerical algorithms used to propagate classical trajectories and to calculate the stability matrix (monodromy matrix) for the HK prefactor we refer to Ref. 19.

Also, it might be advantageous to run several wave packets $c_{n_1}c_{n_2}c_{n_3}(n\tau)$ with different reference states (with different momentum vectors) specified by oscillatory quantum numbers (n_1,n_2,n_3) in order to maximize the weight amplitudes $d_k \sim |\langle \xi|\Psi_k\rangle|^2$ for a certain group of vibrational states. The higher the d_k value is, the better chance the corresponding line will be above the noise/error level. By running different wave packets we aim to collect as many as possible different lines in the spectrum so that if one peak is weak and eliminated by the error reduction procedure from one packet we expect to catch it from another one. We have run four different packets with oscillatory quantum numbers (0,0,0), (1,0,0), (0,0,1), and (0,0,2) and with 5000 trajectories for each. We will label them as 000, 100, 001, and 002, respectively.

Due to the short-range nature of the HK propagator after some time the semiclassical error grows rapidly. It is observed that for all the packets after around a time of 4000 a.u. (corresponding to 400 signal points) the signal starts to show wild oscillations which is an indication of a fast growing error. In Fig. 2 one of the signals is shown in time domain as an example (see the caption for details). Here there is a trade off. By taking a shorter length signal, one obviously reduces resolution and accuracy both in the HI techniques and the Fourier transform. However, a shorter signal contains relatively less error, and so it facilitates the application of Cadzow regularized HI procedure. In further signal processing we set the signal length $N=400$ ($t=4000$ a.u.).

For all of the packets a spectral window of interest has been chosen in the range [344, 34 744] cm^{-1}, which contains $N_w=100$ Fourier grid points, and the band limited signals have been obtained. The inset in Fig. 3 indicates the window of interest. Then, the Cadzow regularized HI spectral estimator has been applied to this signal. As explained in the preceding section, the data matrix C has been constructed and the SVD of C has been calculated. Since the band limited signal had 100 points, the size of the matrices was 50×51. We wish to estimate a rank K of the underlying signal data matrix. In Fig. 1 all the singular values versus their numbers are shown for all the packets. The positions of the gaps taken are shown in the graphs by arrows. The number of singular value points above the gap gives the K value. Cadzow regularized HI signal processing has been applied by taking the K values shown in Fig. 1, and with $N_{\mathrm{iter}}=20$ for each packet.

In Figs. 4 and 5 the Cadzow regularized HI results are

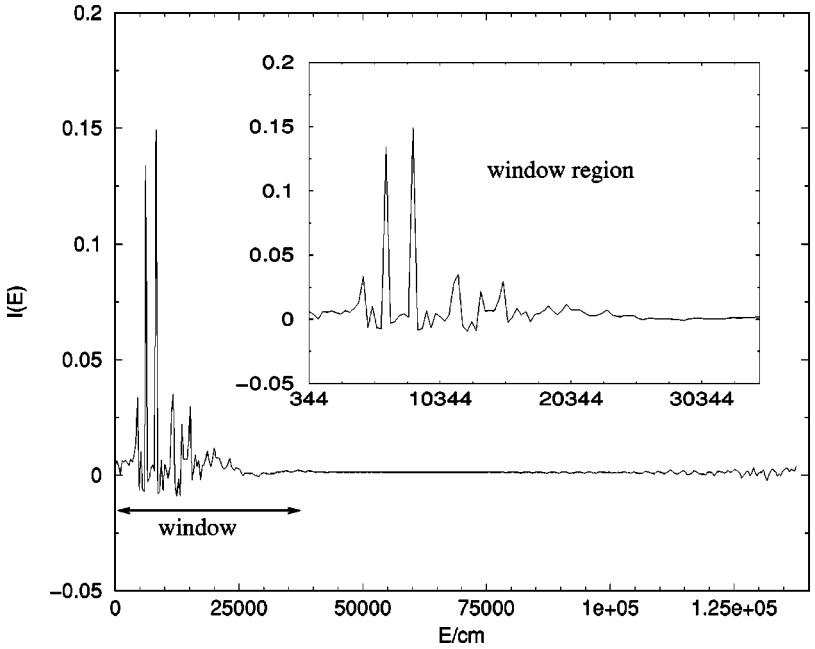

FIG. 3. Real part of the discrete Fourier transform of the signal from packet 000 symmetry A_1 (400 signal points). Region of interest (window) is shown (100 signal points).

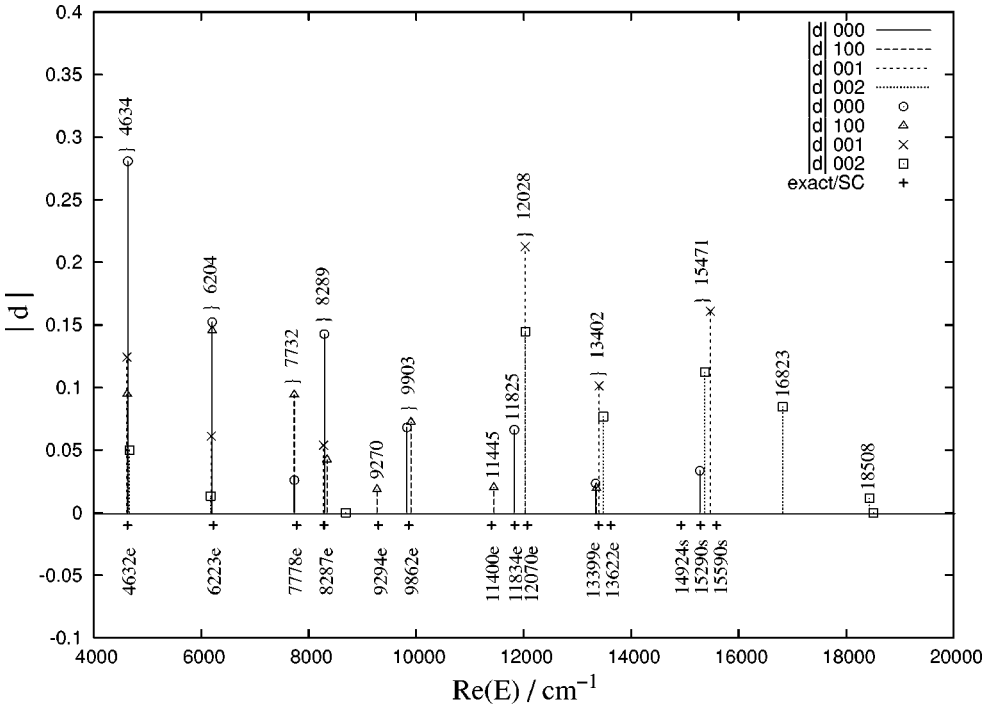

FIG. 4. Stick diagram of $|d_k|$ values from all packets for A_1 symmetry. The numbers having letter "*e*" next to them are exact values of the energies, the numbers having letter "*s*" next to them are SC values of the energies from Ref. 19, the numbers having no letter next to them are real part of the energies of the lines having biggest d_k value in their bundle and obtained by Cadzow regularized HI method by using 5000 trajectories for each packet.

shown for the packets of A_1 and B_2 symmetry, respectively, applied to regularized signals. The heights of the sticks in the diagrams show the $|d_k|$ values and their positions correspond to the real parts of the energies. The symbols are used to indicate to which packet they belong. Dark plus signs up to value 14 000 cm^{-1} are the exact quantum-mechanical energies (marked by letter "*e*"), and the others (marked by letter "*s*") are the SC results from Ref. 19. Some of the lines on the graphs are bundled very closely. These lines are from different packets and we believe that they correspond to the same point in the spectrum. On the figures, a curly bracket sign, "}", is used to indicate a bundle. On the other hand, there are some single lines that can not be ascribed to a bundle and are well separated from the others. These lines

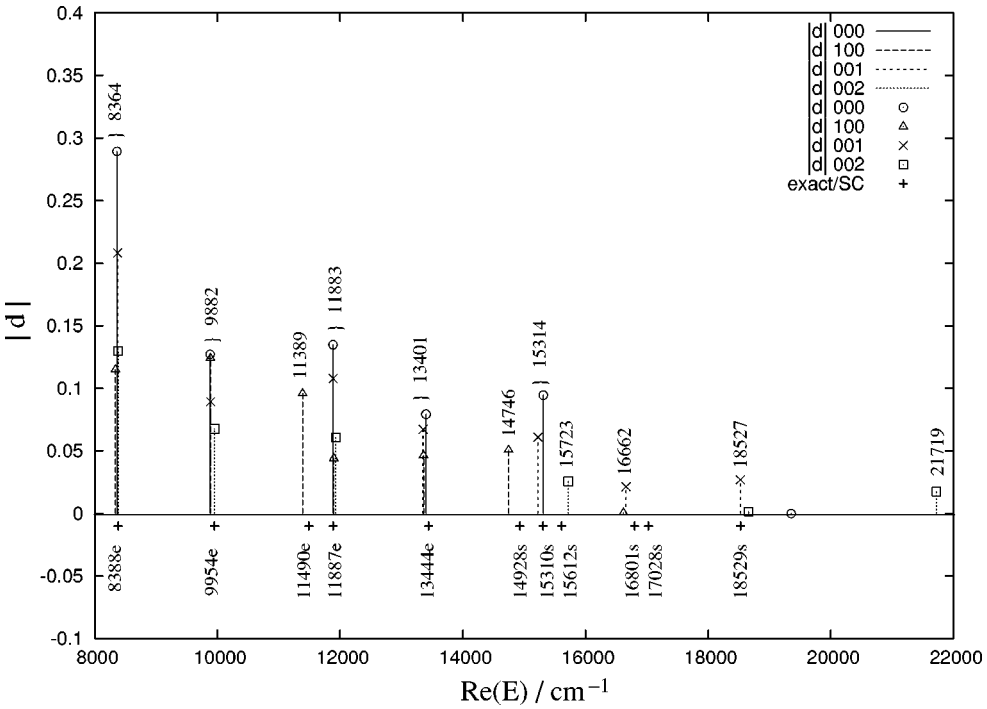

FIG. 5. Stick diagram of $|d_k|$ values from all packets for B_2 symmetry. The other notations are the same as in Fig. 4.

TABLE I. The exact and semiclassical vibrational energies (cm^{-1}) of the water molecule. "*e*" stands for exact energies, "*s*" stands for semiclassical energies from Ref. 19.

Symmetry A_1		Symmetry B_2	
Exact/SC	*E*	Exact/SC	*E*
4632*e*	4634	8388*e*	8364
6223*e*	6204	9954*e*	9882
7778*e*	7732	11 490*e*	11 389
8287*e*	8289	11 887*e*	11 883
9294*e*	9270	13 444*e*	13 401
9862*e*	9903	14 928*s*	14 746
11 400*e*	11 445	15 310*s*	15 314
11 834*e*	11 825	15 612*s*	15 723
12 070*e*	12 028	16 801*s*	16 662
13 399*e*	13 402	17 028*s*	⋯
13 622*e*	⋯	18 529*s*	18 527
14 924*s*	⋯	⋯	⋯
15 290*s*	15 471	⋯	⋯
15 590*s*	⋯	⋯	⋯

are those that are only given by one packet. The number on the top of a stick line is the value of the energy that corresponds to either a single line that does not belong to any bundle or the line that has the highest $|d_k|$ value in a bundle. Since the line with the largest $|d_k|$ value was assumed to be the best converged one, we have selected the energy value of the highest line in a bundle rather than taking their average.

For symmetry A_1 (Fig. 4) we have obtained close results to all the exact energies except the one $E=13\,622\ cm^{-1}$ within a maximum deviation of about 45 cm^{-1}. Around the region of 15 300 cm^{-1} there are three lines that are close to each other within a separation of about 75 cm^{-1}. As compared to the other bundles in the spectrum, this group of three lines has the biggest separation between them. However, since the group itself is well separated from others, we assumed they correspond to the same line in the graph. The other two close lines in this region are missed as compared to the SC results from Ref. 19.

For the symmetry B_2 (Fig. 5) we also obtained results close to the exact ones within a maximum deviation about 100 cm^{-1}. In the energy region higher than 14 000 cm^{-1}, where the exact results are not available, the results are in an agreement with the SC ones from Ref. 19. Only one line is missed in this region.

All the energy values shown on Figs. 4 and 5 are also listed in Table I.

V. CONCLUDING REMARKS

The aim of the work was to make the semiclassical calculation of molecular dynamics problems more practical by reducing the number of trajectories needed in a convergent Monte Carlo averaging procedure. In Ref. 18 and here the use of the Fourier transform of the semiclassically calculated correlation function was replaced by the use of the HI method. The latter method had greater resolution for a given signal length than the Fourier one. This in turn permitted acceptable results to be obtained in Ref. 18 from a shorter propagation time signal. This can be viewed as a first attempt to minimize the error due to the short-range nature of the HK propagator. In general, however, the larger the error, the more trajectories are needed to average it out. In this paper, a second attack was made even more directly on the error with the hope of further reducing the need for the use of excessive number of trajectories.

The noise/error reduction method that has been applied here is based on the Cadzow regularization of the data matrices constructed from the windowed signals. To ensure the effectiveness of the noise/error reduction, short time signals should be collected and averaged until the separation between noise/error and signal singular value points is clear. In practice this may leave some signal points below the noise/error points but at least no noise features will be identified as signal. To recover these "lost" states we take advantage of the fact that the noise/error reduction method, for a given number of trajectories, tends to choose the states with "larger" $|d_k|$ values (i.e., weight factors). By judiciously choosing and semiclassically propagating several initial packets, the lost states can be recovered.

We believe that in total we have satisfied the aim stated at the beginning of this section.

Reference 18 and this paper differ from Refs. 17, 19, and 20, i.e., attempts at converging IVR calculations, by working on the signal and not on the integrand. Combined formulation would be of interest to explore.

ACKNOWLEDGMENTS

The authors thank Professor Chi H. Mak for advice and participation in discussions at the beginning of this work. This work has been supported by NSF Grant No. PHS-0071742.

[1] W. H. Miller, J. Phys. Chem. A **105**, 2942 (2001).
[2] K. G. Kay, J. Phys. Chem. A **105**, 2535 (2001).
[3] D. J. Tannor and S. Garashchuk, Annu. Rev. Phys. Chem. **51**, 553 (2000).
[4] Y. Zhao and N. Makri, Chem. Phys. **280**, 135 (2002).
[5] M. F. Herman and E. Kluk, Chem. Phys. **91**, 27 (1984).
[6] E. J. Heller, J. Chem. Phys. **62**, 1544 (1975).
[7] E. J. Heller, Acc. Chem. Res. **14**, 368 (1981).
[8] J. H. V. Vleck, Proc. Natl. Acad. Sci. U.S.A. **14**, 178 (1928).
[9] S. Tomsovic and E. J. Heller, Phys. Rev. Lett. **67**, 664 (1991).
[10] X. Sun and W. H. Miller, J. Chem. Phys. **108**, 8870 (1998).
[11] M. L. Brewer, J. S. Hulme, and D. E. Manolopoulos, J. Chem. Phys. **106**, 4832 (1997).
[12] V. S. Batista and W. H. Miller, J. Chem. Phys. **108**, 498 (1998).
[13] E. A. Coronado, V. S. Batista, and W. H. Miller, J. Chem. Phys. **112**, 5566 (2000).
[14] M. Thoss, W. H. Miller, and G. Stock, J. Chem. Phys. **112**, 10282 (2000).
[15] A. R. Walton and D. E. Manolopoulos, Mol. Phys. **87**, 961 (1996).
[16] V. I. Filinov, Nucl. Phys. **A271**, 717 (1986).
[17] N. Makri and W. H. Miller, Chem. Phys. Lett. **139**, 10 (1987).
[18] F. Grossman, V. A. Mandelshtam, H. S. Taylor, and J. S. Briggs, Chem. Phys. Lett. **279**, 355 (1997).
[19] A. L. Kaledin and W. H. Miller, J. Chem. Phys. **118**, 7174 (2003).
[20] A. L. Kaledin and W. H. Miller, J. Chem. Phys. **119**, 3078 (2003).
[21] J. Main, P. A. Dando, D. Belkic, and H. S. Taylor, J. Phys. A **33**, 1247 (2000).
[22] J. A. Cadzow, IEEE Trans. Acoust., Speech, Signal Process. **36**, 49 (1988).
[23] S. D. Kunikeev and H. S. Taylor, J. Phys. Chem. A **108**, 743 (2004).
[24] W. H. Press, B. P. Flannery, S. A. Teukolsky, and W. T. Vetterling, *Numerical Recipes: The Art of Scientific Computing*, 2nd ed. (Cambridge University Press, Cambridge, 1992).
[25] G. H. Golub and C. V. Loan, *Matrix Computations*, 3rd ed. (Johns Hop-

kins University Press, 1996).
[26] Y. Li, K. J. R. Liu, and J. Razavilar, IEEE Trans. Signal Process. **45**, 481 (1997).
[27] F. R. Gantmacher, *The Theory of Matrices* (Chelsea, New York, 1974).
[28] E. B. Wilson, J. C. Decius, and P. C. Cross, *Molecular Vibrations* (McGraw-Hill, New York, 1955).
[29] J. K. G. Watson, Mol. Phys. **15**, 479 (1968).
[30] J. M. Bowman, A. Wierzbicki, and J. Zuniga, Chem. Phys. Lett. **150**, 269 (1988).
[31] K. Husimi, Proc. Phys. Math. Soc. Jpn. **22**, 264 (1940).